2.1 Introduction

This chapter presents the details of synthesis of phase pure nanocrystalline BF-xPT solid solutions in the composition range of $0.20 \leq x \leq 0.50$, using chemical route. The synthesis of pure phase $BiFeO_3$ powders is one the most challenging work because of the narrow temperature range in which $BiFeO_3$ stabilizes and formation of a number of unwanted phases of Bi and Fe oxides, like $Bi_{36}Fe_2O_{57}$ [Pradhan (2005)], $Bi_2Fe_4O_9$ [Kumar et al. (2000)], $Bi_{25}FeO_{39}$ [Lebeugle et al. (2007)] and $Bi_{46}Fe_2O_{72}$ [Tabres-Munoz (1985)].These impurity phases appear if temperature is not controlled accurately. Some researcher have attempted to leach out these secondary phases, formed during synthesis of $BiFeO_3$ by dilute nitric acid [Sosnowska et al. (1982); Kumar et al. (2000); Lebeugle et al. (2007); Arnold et al. (2009)]. However such removal process may disturb the overall stoichiometry of primarily intended $BiFeO_3$. Synthesis of $BiFeO_3$ has been reported using several other chemical techniques. For example synthesis by microwave-hydrothermal technique has been reported by Komarneni et al. (1996). Wang et al. (2004) and Pradhan et al. (2005) prepared phase pure $BiFeO_3$ ceramics by a rapid liquid-phase sintering technique. Gosh et al. (2005) have prepared pure $BiFeO_3$ nano crystalline powders by the tartaric acid based sol-gel method coupled with additional calcination process. A few other workers have prepared $BiFeO_3$ by hydrothermal method [Chen et al. (2006), Wei et al. (2012), also.

Forming a solid solution of $BiFeO_3$ with other ABO_3 type of perovskites not only helps to reduce the formation of impurity phases but also enhances the resistivity, multiferroic properties and magnetoelectric coupling [Smith et al. (1968); Kanai et al. (2001); Jun et al. (2005); Wang et al. (2005); Li et al. (2007); Bhattacharjee et al. (2010)]. Park et al.(2010) synthesized $BiFeO_3$-$BaTiO_3$ by solid state rout, which significantly enhanced

the magnetic property of $BiFeO_3$. The present thesis deals with one of such solid solution system.

2.2 Characterization tools

2.2.1 X-ray diffraction

X-ray diffraction technique is used to characterize and identifying the different phases present in any material. The simplicity and advantage of x-ray powder diffraction method can be given as follows (i) the powder diffraction pattern is characteristic of a given substance, (ii) each substance in a mixture produces its own pattern independent of others and (iii) the method is capable of quantitative and qualitative analysis of the phases present in a given mixture. In the present case, the calcined and sintered powders were characterized for the presence of different phases in the BF-xPT compositions synthesized during this thesis work. X-ray diffraction measurements were carried out using an 18 kW rotating anode (Cu Kα) based Rigaku (RINT 2000/ PC series) powder diffractometer operating in the Bragg Brentano geometry and fitted with a graphite monochromator in the diffracted beam.

Some of the compositions are characterized through Synchrotron x-ray diffraction (SXRD). These SXRD patterns were collected at high resolution powder diffraction beamline P02.2 at PETRAIII, DESY, Hamburg, Germany for resolving the controversy about the structure. The wavelength for the synchrotron x-ray diffraction (SXRD) used was0.2079 Å

2.2.2 TGA/DTA Characterization

Differential thermal analysis (DTA) and thermogravimetric analysis (TGA) have been performed in temperature range of 300 to 600 °C using simultaneous TGA/DTA Mettler

instrument. The sample placed in the Alumina crucible was heated at a rate of 10 °C /min in inert nitrogen atmosphere.

2.2.3 Scanning electron microscope (SEM) and energy dispersive x-ray analysis (EDX)

The microstructure (grain size) was characterized using a field emission gun based scanning electron microscope (SEM) (Supra 40, Zeiss, Germany), equipped with energy dispersive x-ray analyzer and with Nova NanoSEM 450. The pellet was washed in etchant solution of 100 ml (5%HCL+ 10%HNO_3+85% Distilled water) for better results .Then the sintered pellets were coated with conducting gold film by sputtering under vacuum before recording SEM pictures. Varied amount of gun voltage was applied during the SEM analysis to produce the good contrast in the images. Compositional analysis was carried out by Energy dispersive x-ray spectroscopy (EDX) available with the above mentioned SEM. Its characterization principle is that each element has a unique atomic structure allowing emission of x-rays that are characteristic of that element's atomic structure which is distinguishable from the x-ray emitted by another element, by and large.

2.3 Synthesis of BF-xPT

BF-xPT compositions with general formula BF-xPT with x in the range $0.20 \leq x \leq 0.50$ has been synthesized through sol-gel route. The conditions and sequences used in the sample preparation are as follows:

2.3.1 Sample preparation techniques

The nanocrystalline BF-xPT solid solutions powders were synthesized by sol-gel route which are given elsewhere [Singh (2001)]. The ingredients used for the synthesis are ferric nitrate (≥99.5% Sigma Aldrich), lead nitrate (≥99.0% Sigma Aldrich), bismuth

nitrate (≥99.9% Sigma Aldrich) and titanium isopropoxide (≥97.0% Sigma Aldrich). These stoichiometric amounts of metal nitrate (iron, lead and bismuth) aqueous solutions and ethylene glycol (EG) stabilized titanium isopropoxide solution were mixed together at 60 °C. In order to avoid any precipitation of TiO_2 by moisture or air (i) EG has been taken 7 times by volume as compared to the volume of titanium isopropoxide solution and (ii) the pH was adjusted between 1 and 2. This mixed solution was added slowly to the aqueous solution of maleic acid kept at 60 °C and the resultant solution was stirred continuously to ensure complexation of metal cations. The solution was then heated to 80 °C to initiate evaporation of water and polymerization. The overnight heating of the sample resulted in a brown coloured gel. The excess ethylene glycol present in the gel was dried at 150-170 °C, leaving behind a dark-brown dried polymer precursor. The precursor was then calcined at 550 °C for 6 hours, in a closed environment. Detail process of synthesis is given in flow chart (see fig. 2.1).

2.4 Optimization of calcination temperature

Differential thermal analysis (DTA) and thermogravimetric analysis (TGA) can give an idea about underlying processes happening during the growth of a system. Fig.2.2 shows the TGA and DTA curves of BF-xPT precursor powders. It is seen from TGA curve that, below 150 °C there was a weight loss of ~ 4%, which was indicative of the evaporation of the trapped moisture in the sample. A dominant weight loss of about 42% has occurred between 300 °C and 450 °C. This change in the weight loss can generally be attributed to a combustion-like reaction in which organic molecules acting as fuel and nitrate ions as oxidizing agent burning off. This process is continuing up to the temperature ~450 °C. Between 450 °C to 600 °C there is no major change in the weight of the sample reflecting the completion of combustion reaction. We have a selected a temperature well above the

reaction completion temperature as calcinations temperature (i.e. 550 ^{o}C) to get single phase samples. The details of sample sintering temperature and its role on size of nanocrytalline powder are discussed in the next section of this chapter.

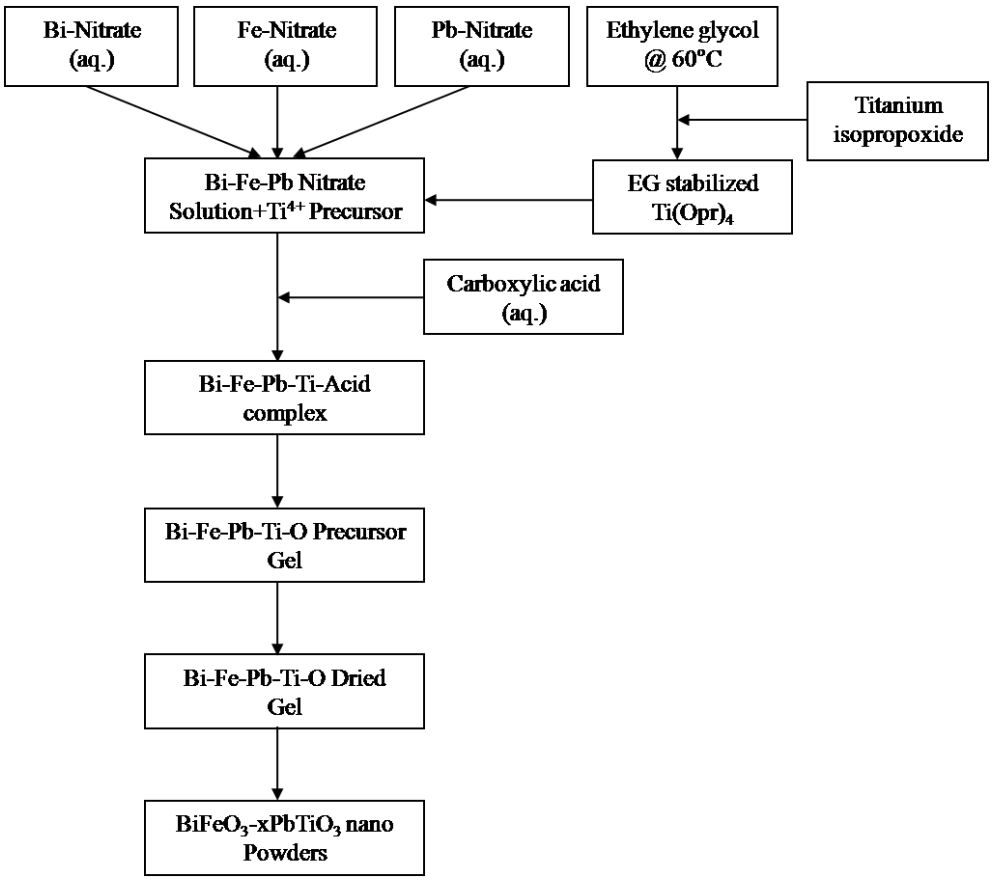

Fig. 2.1 Flow chart for the preparation of (1-x) BF-xPT samples using Sol-gel method.

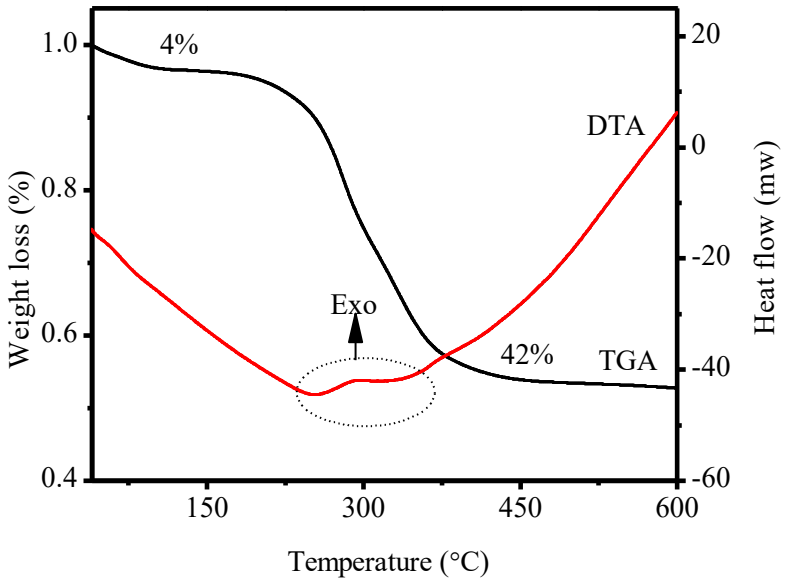

Fig.2. 2 Differential thermal analysis and thermogravimetric analysis curve of dried gel powder of BF-xPT sample for x=0.50.

2.5 Optimization of chelating agent

A chelating agent is a material whose molecules can form several bonds to the metal ion. Different chelating agents have been tried to get a sample free from secondary phase. Figure 2.3 shows the X-ray diffraction pattern of the powder calcined at 550 °C for all three chelating agents (Tartaric acid, Malic acid, Maleic acid). There are impurities phases present, where tartaric and malic acid has been used. These phases have been identified as $Bi_{25}FeO_{40}$ (JCPDS 46-0416) and $Bi_2Ti_2O_7$ (JCPDS 32-0118) for the samples formed using tartaric acid and malic acid as chelating agent respectively as marked in fig. 2.3 with asterisk. A similar finding was reported by [Sebach et. al (2007)], as well where a small amount of impurity phase always remained after the calcinations. As confirmed by x-ray analysis that the formation of pure phase of BF-0.50PT only when Maleic acid is used as chelating agent.

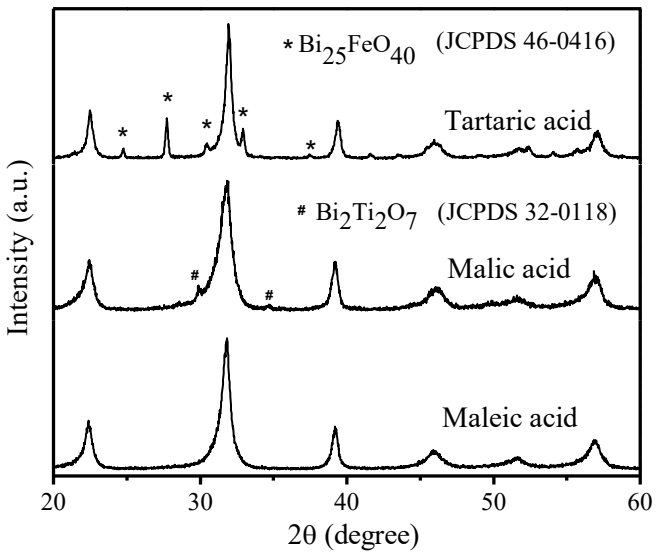

Fig. 2.3 X-ray diffraction pattern for BF-0.5PT samples using different chelating agent.

2.6 Optimization of calcination temperature

From the TGA/DTA analysis, it is shown that dried gel decomposes at 450℃, so we have calcined one of the synthesized dried gel at 450℃ and onwards. The x-ray diffraction patterns of BF-0.5PT powders calcined at different temperatures is shown in Fig. 2.4. The x-ray diffraction pattern collected at 450℃ was indexed using JCPDS files (46-0416). The major components of XRD pattern has been indexed as a main perovskite peaks of BF-0.50PT along with one minor phases of $Bi_{25}FeO_{40}$.The reflections of the impurity phase is indicated by specific symbols as shown in Fig. 2.4. As we see from the figure the dried gel calcined at 450℃ and 500℃ have impurity phase as well as some un-decomposed compound.

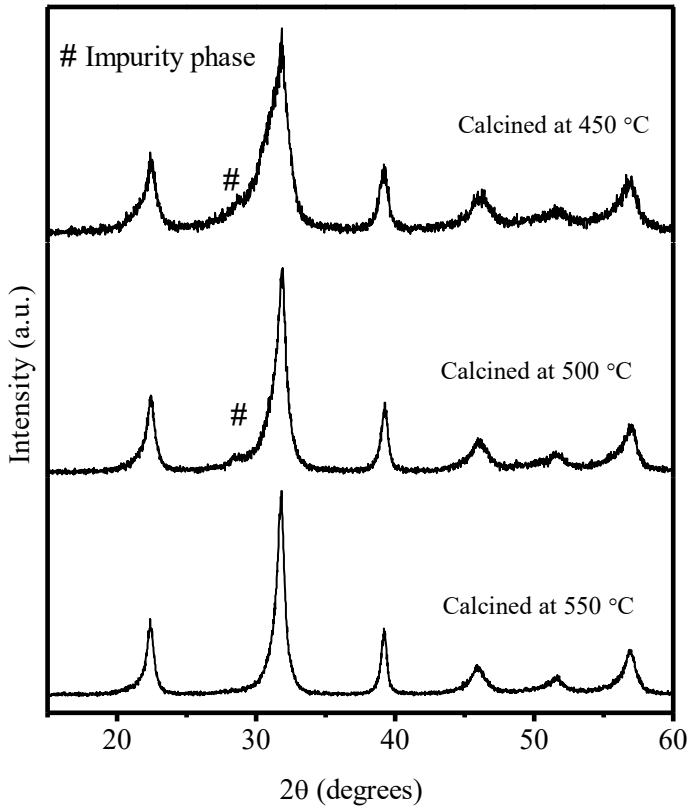

Fig. 2.4 X-ray diffraction pattern for BF-0.5PT calcined at different temperatures

The x-ray diffraction pattern of dried gel calcined at 550℃ shows sharp and well indexed perovskite peak without any impurity. So, we use this calcination temperature for synthesis of BF-xPT, taking x=0.20, 0.25, 0.30, 0.35, 0.40 and 0.50. The XRD patterns for the as calcined powder for six compositions are shown in Fig. 2.5. From this figure it is clear that for composition with x=0.2 and 0.25, have another two crystalline peaks beside of main perovskite peak. As per early literature (discussed in chapter I) this composition has been reported to lie far away from morphotropic phase boundary, which consist both tetragonal and monoclinic phase. The most intense peak is marked as monoclinic phase whereas lowest intense peak marked as tetragonal phase. The

prominent peaks of these two compositions are not splitted, which indicates its poor crystallinity.

2.7 Preparation of Green Pellets

After calcination, the sample was properly crushed and mixed with an organic binder of 2% polyvinyal alcohol (PVA) solution in an agate mortar. PVA mixed powder was used for the preparation of green pellets. A cylindrical steel die of 12 mm diameter was used to make green pellets of BF-xPT sample. Then die containing powder was uniaxially pressed at an optimized pressure (for getting maximum green density) of 65 kN in a hydraulic press. The green pellets were kept on alumina plate and kept in a furnace at 500°C for 10 hours to burn off the binder material polyvinyl alcohol (PVA).

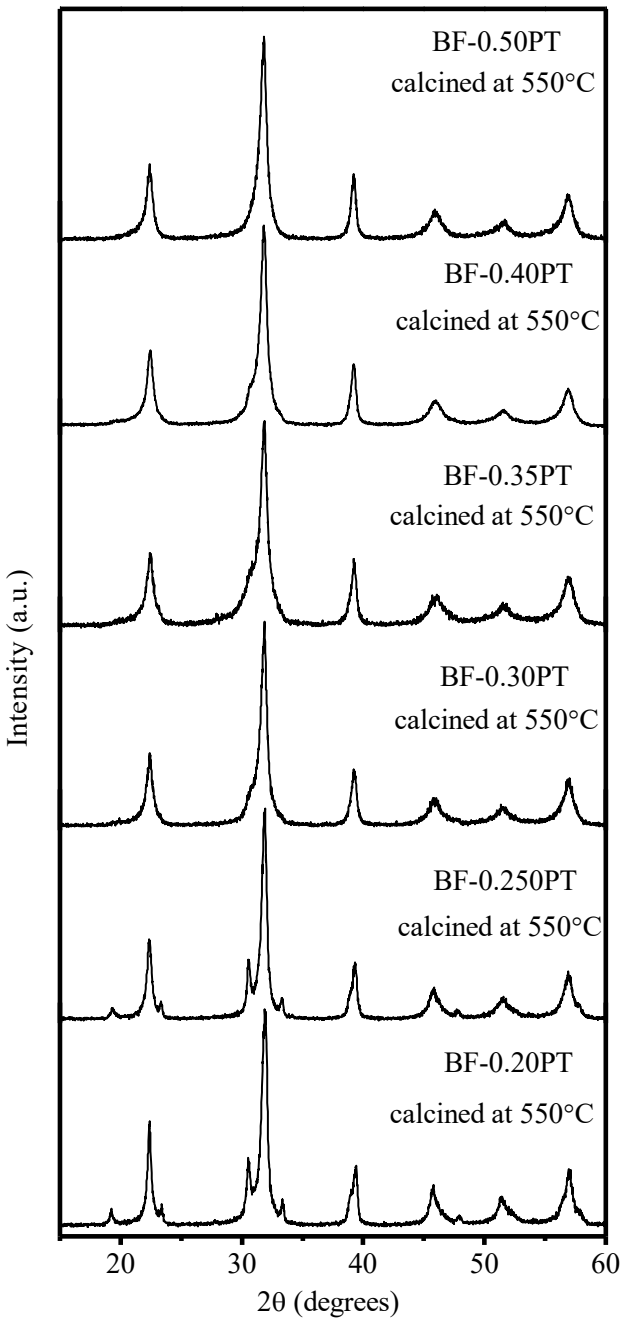

Fig. 2.5 X-ray diffraction pattern for BF-xPT (x=0.2 to 0.5) calcined at 550℃.

2.8 Sintering

To synthesize different sizes of BF-xPT, we sintered the green pellets at different temperature. For that we have categorized our sintering process three ways: (a) Synthesis of different sizes of BF-xPT above MPB (i.e. $x \geq 0.31$), (b) Synthesis of different sizes of BF-xPT below MPB (i.e. $x \leq 0.27$) and (c) Synthesis of different sizes of BF-xPT within MPB (i.e. $0.31 \leq x \geq 0.27$).

2.9 Synthesis of different sizes of BF-xPT above MPB (x=0.50, 0.40 and 0.35)

Sintering of the PVA evaporated pellets was carried in a closed alumina crucible sealed with MgO powder in the different temperature range of 550°C to 1050°C for 6 hours. Bi_2O_3 atmosphere was maintained inside the closed alumina crucible by keeping suitable amount of the calcined powder of the same composition inside the closed alumina crucible as a spacer powder. For x-ray and other characterization, the sintered pellets were crushed into fine powders and then annealed at 500°C for 10 hours to remove the strain introduced during crushing. These processes are applicable for all compositions which are above the MPB region (i.e $x \geq 0.31$). Fig. (2.6 to 2.8) shows x-ray diffrection pattern for BF-0.5PT, BF-0.40PT and BF-0.35PT compostions sintered at different temperatures.

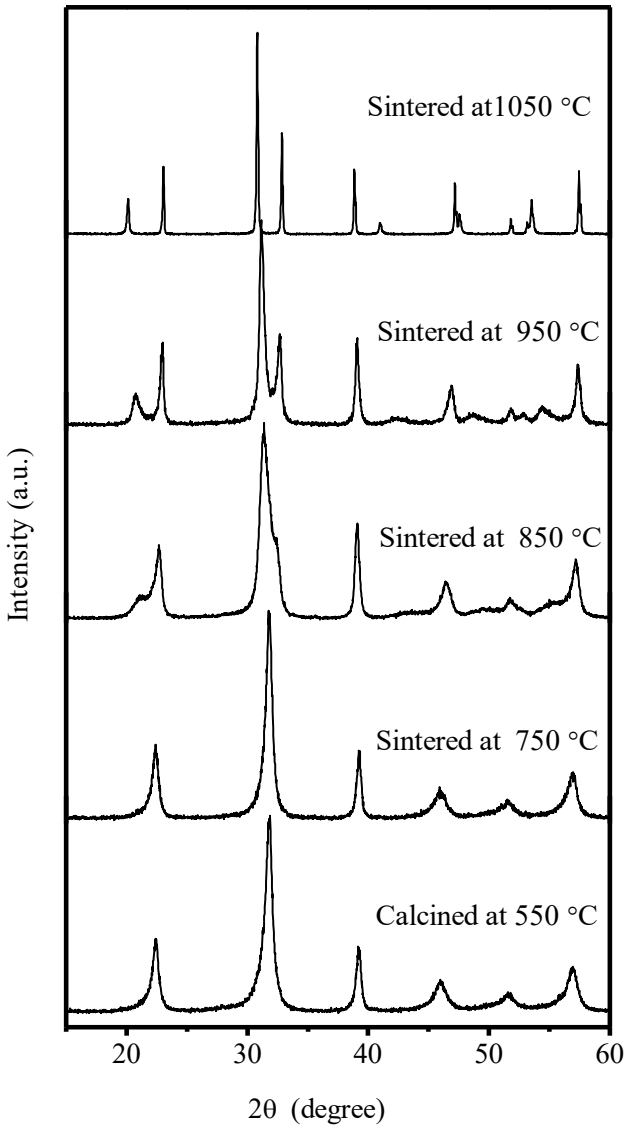

Fig. 2.6 Room temperature x-ray diffraction pattern of BF-0.5PT calcined at 550℃ and sintered at different temperatures.

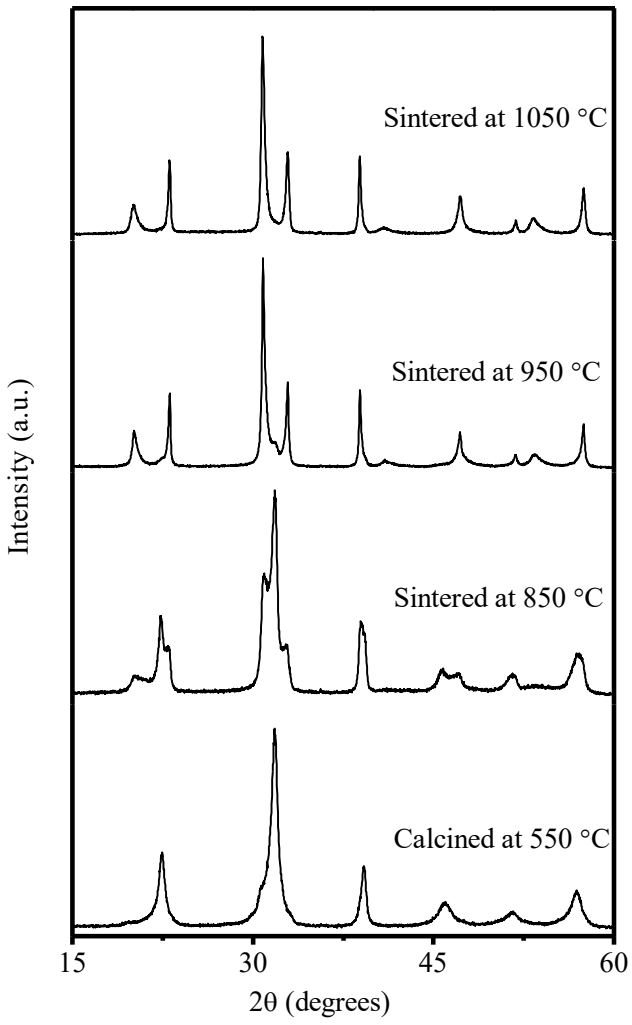

Fig. 2.7 Room temperature x-ray diffraction pattern of BF0.40PT calcined at 550℃ and sintered at different temperatures.

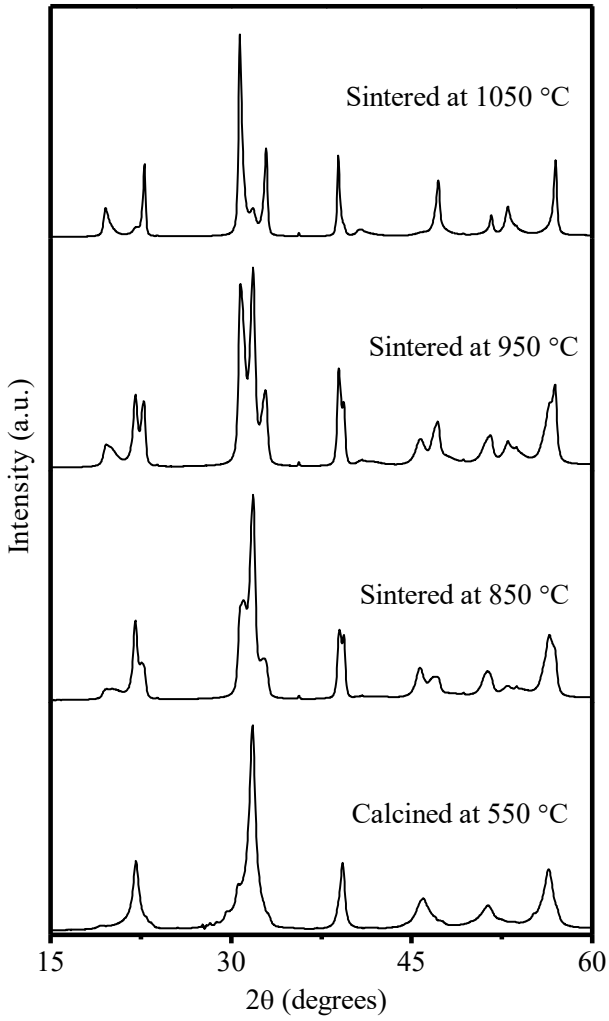

Fig. 2.8 Room temperature x-ray diffraction pattern of BF0.35PT calcined at 550℃ and sintered at different temperatures.

2.10 Synthesis of different sizes of BF-xPT below MPB (x=0.25 and 0.20)

2.10.1 Optimization of sintering temperature forBF-0.25PT powder

For the optimization of the synthesis parameters, the BF-xPT composition with x=0.25 was selected. On behalf of literature survey, this composition has been reported to lie below the morphotropic phase boundary. As we see from fig 2.9, that there are some extra peaks are present beside of pure monoclinic peak. Bhattacharjee et al. reported that these

peaks nothing but peaks of tetragonal phase which is developed through crushing of powder. As we crushed the calcined powder in mortar pastel, the intensity of tetragonal peaks increased which is shown in fig. 2.9(b). The crushed powder and some adhesive like PVA are mixed together in mortar pastel for making pellets. These pellets are sintered in a closed alumina crucible sealed with MgO powder at the temperature of 1000℃ for 6 hours. X-ray pattern of sintered pellet was shown in fig. 2.9(c), which shows pure single phase monoclinic peaks. For x-ray and some other characterization sintered pellets were carefully crushed into fine powders in an agate mortar using agate pestle for five minutes. After crushing again tetragonal peaks are developed in the sample which is confirmed by XRD. The crushed powder is then annealed at 700 ℃ for 10 hours to remove the mechanical strains and tetragonal phase induced during crushing of the sintered pellets. No liquid medium was used during crushing in all the studies described in this paper. Annealing below 700 ℃ is not effective in removing the stress induced tetragonal phase. Special precaution is to be taken in the annealing process, as the crushed powder particles may conglomerate during annealing at high temperatures making the annealed powder unsuitable for powder XRD analysis without further crushing. To avoid the conglomeration of powder particles, crushed powder (~1 gm in weight) is spread out on a circular alumina sheet (10 cm diameter) so as to form a thin layer of powder. This reduced the possibility of the powder particles getting conglomerated. To obtain different sizes of BF-0.25PT, the pellet was sintered at four different temperatures ranging from 1000℃ to 700℃. Sintering below 700℃ shows two phase structure, so it restrict us to sinter below this temperature.

So for the synthesis of pure BF-0.25PT and BF-20PT powder of different sizes, we sintered it at four different temperatures ranging from 1000℃ to 700℃ (see fig.2.10 and 2.11).

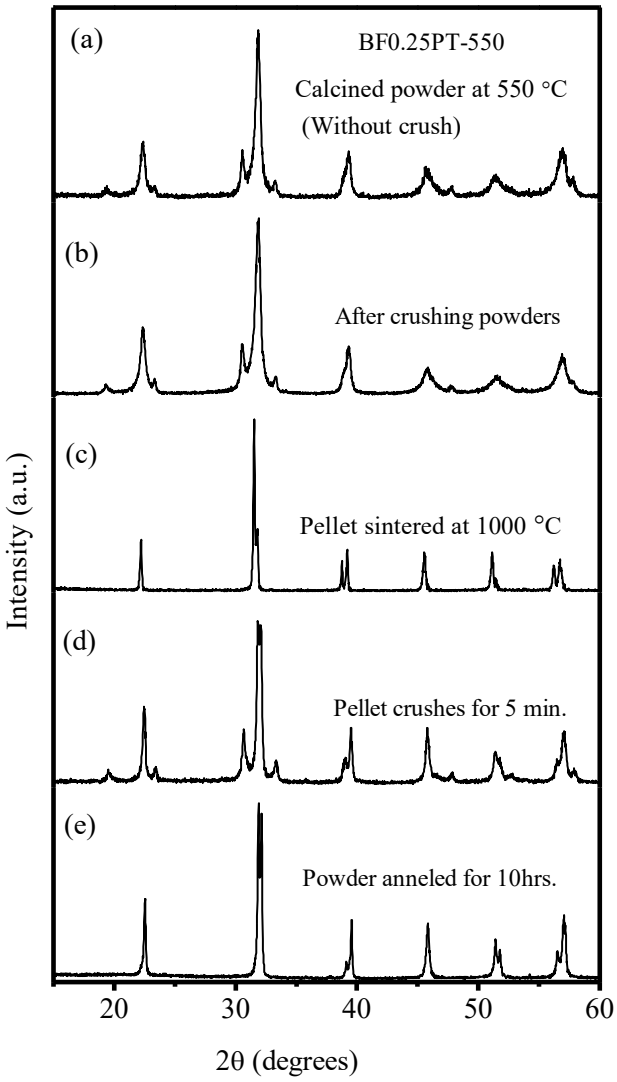

Fig. 2.9 Room temperature x-ray diffraction pattern of BF0.25PT for optimization of sintering temperature.

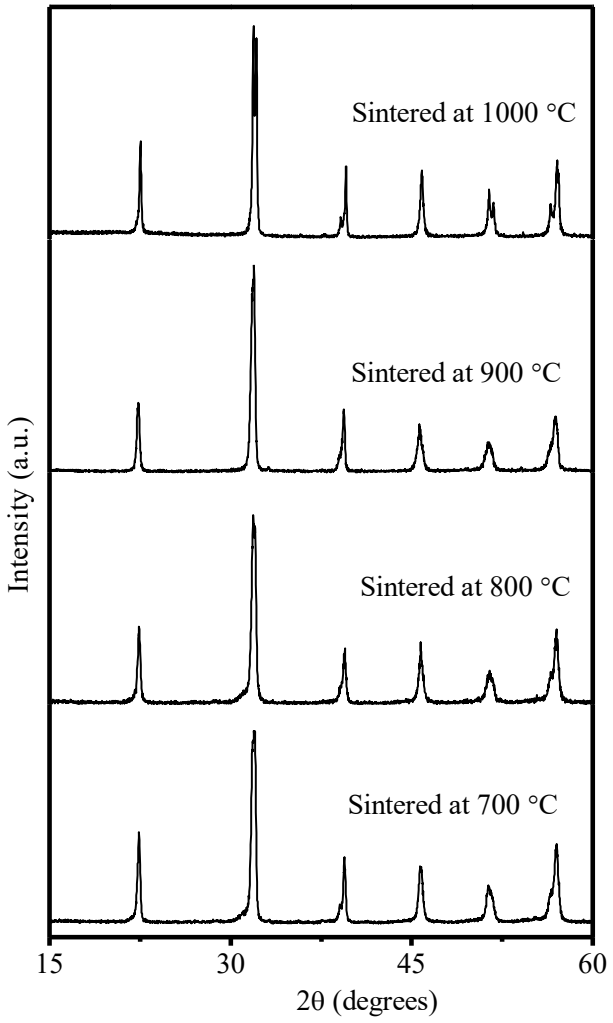

Fig. 2.10 Room temperature x-ray diffraction pattern of BF0.25PT sintered at different temperatures.

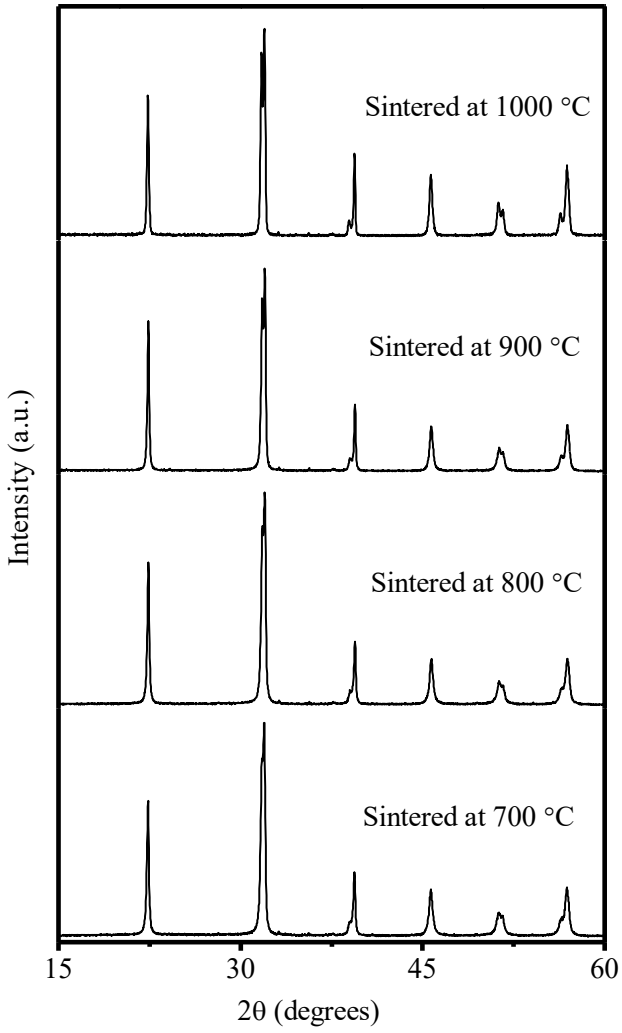

Fig. 2.11 Room temperature x-ray diffraction pattern of BF0.20PT sintered at different temperatures.

2.11 Synthesis of different sizes of BF-xPT within MPB (x=0.30)

For the synthesis of different size of BF-0.3PT, same process was adopted as for BF-0.20PT and BF-0.25PT.

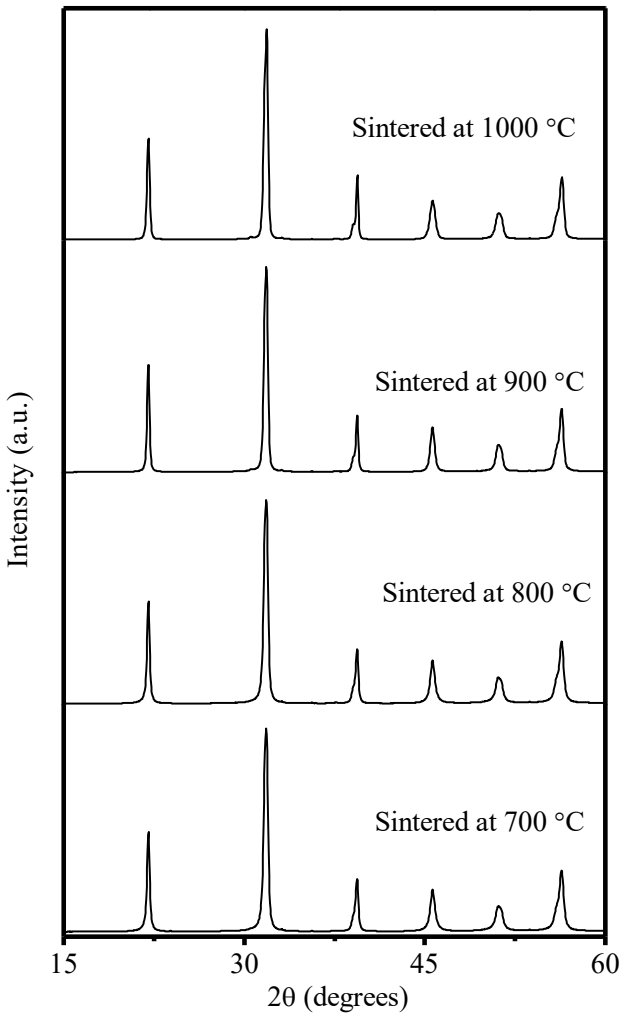

Fig. 2.12 Room temperature x-ray diffraction pattern of BF0.30PT sintered at different temperatures.

2.12 Microstructural and compositional studies for BF-xPT

Scanning electron microscopic analysis was done on the sintered pellets to determine the grain size of the samples and uniformity of the sample matrix of BF-xPT powder. EDX analysis was carried out to confirm the chemical compositions of the synthesized samples. Fig.(2.13 to 2.19) depicts the scanning electron micrographs and EDX spectrums of BF-xPT (x=0.20,0.25,0.30,0.35,0.40 and 0.50) ceramics for some selected area. The average grain size was found to effectively growing with increasing sintering temperature. The average grain size was determined by averaging over more than 30 particles in different regions of the microstructure. The average grain size of the different samples is listed in Tables (2.1 to 2 .7).

EDX spectra of BF-xPT shows that each sample is composed of bismuth (Bi), lead (Pb), iron (Fe), titanium (Ti) and oxygen (O) atoms. Since, the oxygen atom is very less sensitive to the x-ray diffraction due to low atomic scattering factor (low atomic number Z = 8), the average atomic percentage of oxygen atom can not be determined accurately from the EDX spectrum. This inaccuracy in atomic percent of oxygen atoms also disturbs the atomic percentages of other atoms (Bi, Pb, Fe and Ti). Therefore, in order to examine the composition (x) of the synthesized BF-xPT solid solutions more accurately, the EDX analysis was carried out for Bi, Fe, Pb and Ti only ignoring oxygen.

2.12.1 Microstructural and compositional studies for BF-0.5PT

The average size and sintering temperatures are given in Table 2.1. The minimum particle size has been found to be ~18 nm whereas the largest size is ~120 nm corresponding to the sintering temperatures of 550 and 1050 ^{0}C, respectively. Representative EDX spectrum of each sample is shown on the right side column of SEM image. Its analysis for heavy elements (Bi, Pb, Ti and Fe), as collected from 6 to 8 different regions, confirmed

that the average composition of all the sizes corresponds to the nominal composition range.

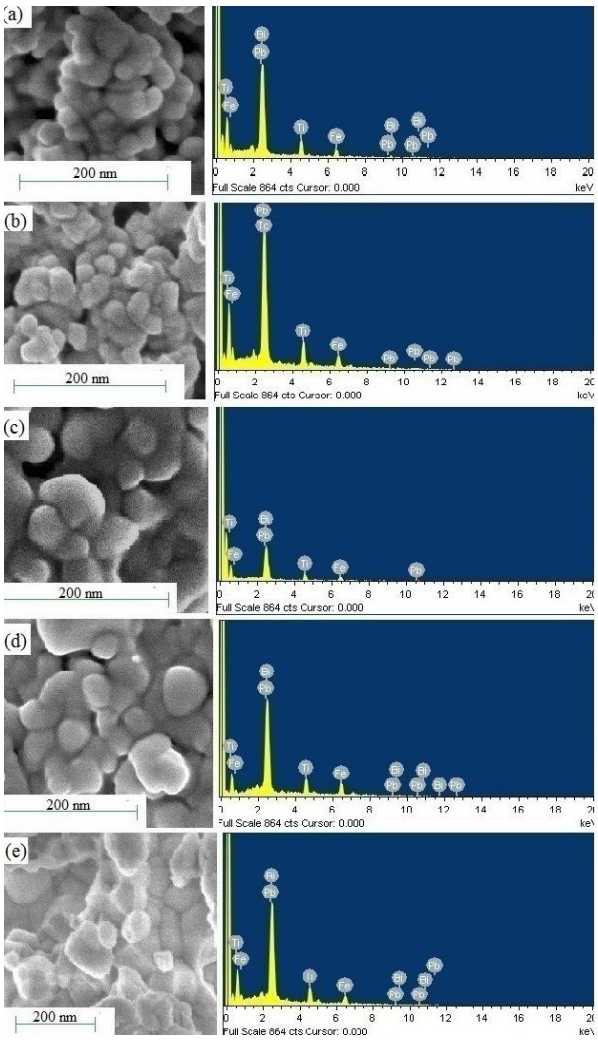

Fig. 2.13 Scanning electron micrographs and EDX spectra of BF -0.5PT powder sintered at (a) 550℃ (b) 750℃ (c) 850℃ (d) 950℃ (e) 1050℃

Table 2.1 Estimated particle size and results of EDX analysis of BF-0.50PT samples

Element	Estimated sizes BF-0.5PT from SEM				
	Clacined at 550℃	Sintered at 750℃	Sintered at 850℃	Sintered at 950℃	Sintered at 1050℃
	18 nm	21nm	31nm	45nm	120nm
	Atomic(%) from EDX				
Bi	26.04	24.22	25.33	25.81	25.74
Fe	23.71	25.36	24.33	23.67	23.75
Pb	24.37	22.95	23.49	24.10	21.93
Ti	25.88	27.47	26.85	27.47	28.58
BF:PT	49.75:50.25	49.58:50.42	49.66:50.34	49.48:50.52	49.49:50.51

2.12.2 Microstructural and compositional studies for BF-0.4PT

The average size and sintering temperatures are given in Table 2.2. The minimum particle size has been found to be ~40 nm for sample calcined at 550℃, whereas the largest size is ~350 nm corresponding to the sintering temperatures of 1050 ^{0}C. Representative EDX spectrum of each sample is shown on the right side column of SEM image. Its analysis confirmed that the average composition of all the sizes corresponds to the nominal composition range.

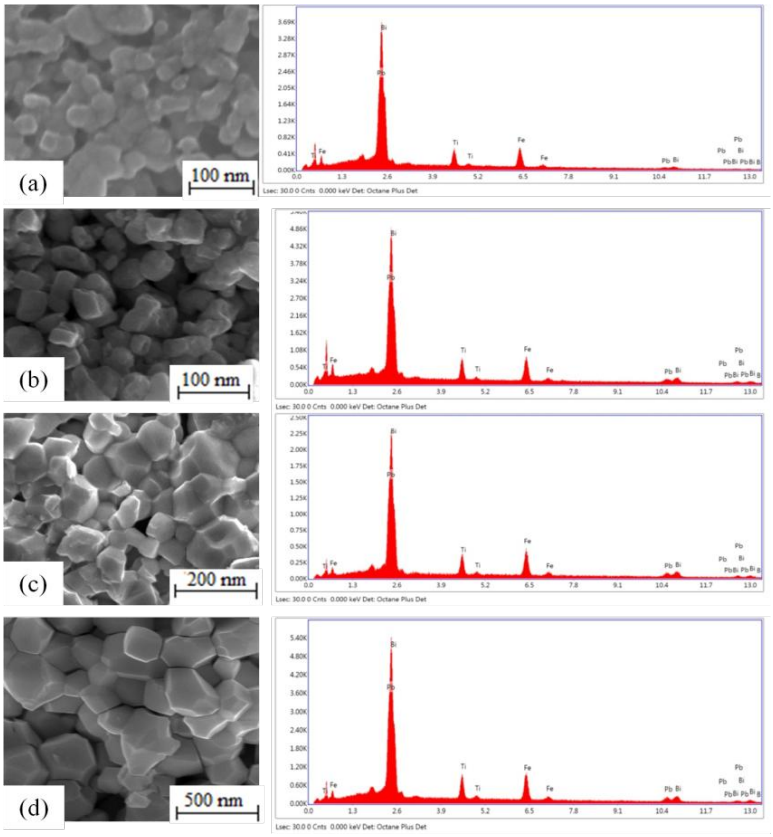

Fig. 2.14 Scanning electron micrographs and EDX spectra of BF -0.4PT powder sintered at (a) 550℃ (b) 850℃ (c) 950℃ (d) 1050℃.

Table 2.2 Estimated particle size and results of EDX analysis of BF-0.40PT samples

Element	Estimated sizes BF-0.4PT from SEM			
	Clacined at 550℃	Sintered at 850℃	Sintered at 950℃	Sintered at 1050℃
	40 nm	60nm	110nm	350nm
	Atomic(%) from EDX			
Bi	34.23	32.30	32.42	32.21
Fe	26.49	27.52	27.82	27.90
Pb	15.07	19.80	17.28	18.75
Ti	24.21	20.38	21.48	21.14
BF:PT	60.72:39.28	59.82:40.18	60.24:39.76	60.11:39.89

2.12.3 Microstructural and compositional studies for BF-0.35PT

The average size and sintering temperatures are given in Table 2.3. The minimum particle size has been found to be ~42 nm for sample calcined at 550℃, whereas the largest size is ~750 nm corresponding to the sintering temperatures of 1050 ^{0}C. Representative EDX spectrum of each sample is shown on the right side column of SEM image. Its analysis confirmed that the average composition of all the sizes corresponds to the nominal composition range.

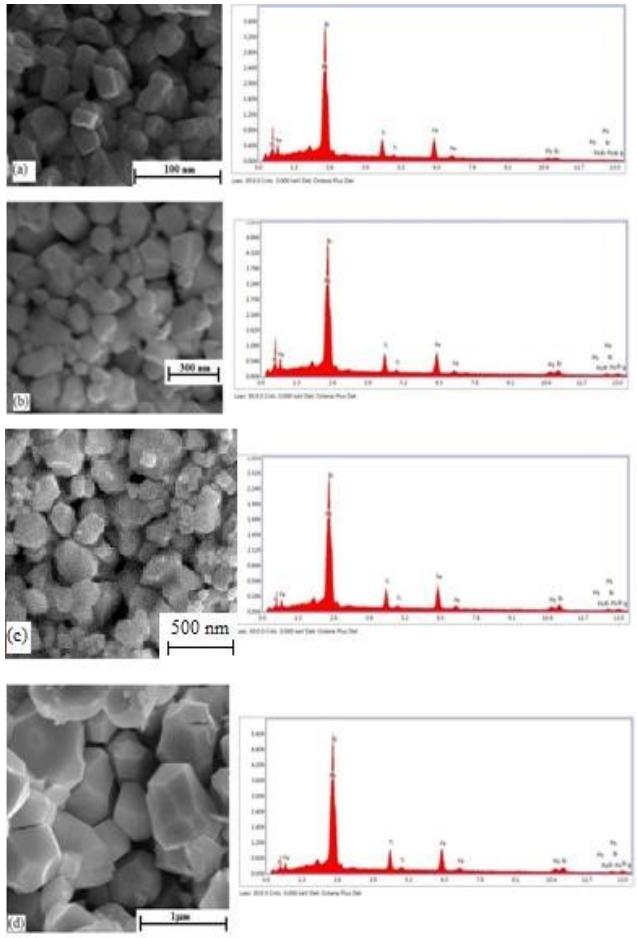

Fig. 2.15 Scanning electron micrographs and EDX spectra of BF -0.35PT powder sintered at (a) 550℃ (b) 850℃ (c) 950℃ (d) 1050℃.

Table 2.3 Estimated particle size and results of EDX analysis of BF-0.35PT samples .

Element	Estimated sizes BF-0.35PT from SEM			
	Clacined at 550℃	Sintered at 850℃	Sintered at 950℃	Sintered at 1050℃
	42 nm	150nm	300nm	750nm
	Atomic(%) from EDX			
Bi	49.25	48.52	47.28	47.95
Fe	15.96	16.85	17.63	17.45
Pb	25.94	26.10	26.23	25.57
Ti	8.85	8.54	8.85	9.03
BF:PT	65.21:34.79	65.37:34.63	64.91:35.09	65.4:34.6

2.12.4 Microstructural and compositional studies for BF-0.3PT

The average size and sintering temperatures are given in Table 2.4. The minimum particle size has been found to be ~100 nm for sample sintered at 700℃, whereas the largest size is ~1μm corresponding to the sintering temperatures of 1000 ^{0}C. Representative EDX spectrum of each sample is shown on the right side column of SEM image. Its analysis confirmed that the average composition of all the sizes corresponds to the nominal composition range.

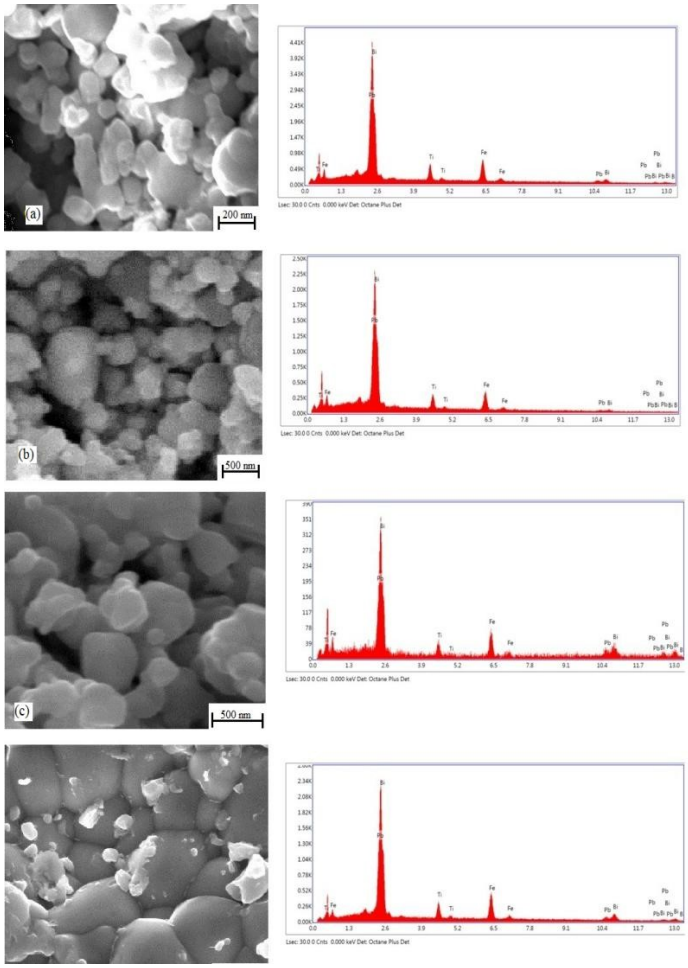

Fig. 2.16 Scanning electron micrographs and EDX spectra of BF -0.30PT powder sintered at (a) 700℃ (b) 800℃ (c) 900℃ (d) 1000℃

Table 2.4 Results of EDX analysis of BF-0.30PT samples with different sizes.

Element	Estimated sizes BF-0.30PT from SEM			
	Clacined at 700℃	Sintered at 800℃	Sintered at 900℃	Sintered at 1000℃
	100nm	220 nm	380 nm	1 μm
	Atomic(%) from EDX			
Bi	50.87	55.01	49.47	51.76
Fe	19.02	15.31	21.37	18.38
Pb	23.51	22.77	22.87	21.95
Ti	6.60	6.91	6.29	7.91
BF:PT	69.89:30.11	70.32:29.68	70.84:29.16	70.14:29.86

2.12.5 Microstructural and compositional studies for BF-0.25PT

The average size and sintering temperatures are given in Table 2.5. The minimum particle size has been found to be ~150 nm for sample sintered at 700℃, whereas the largest size is ~2µm corresponding to the sintering temperatures of 1000 ^{0}C. Representative EDX spectrum of each sample is shown on the right side column of SEM image. Its analysis confirmed that the average composition of all the sizes corresponds to the nominal composition range.

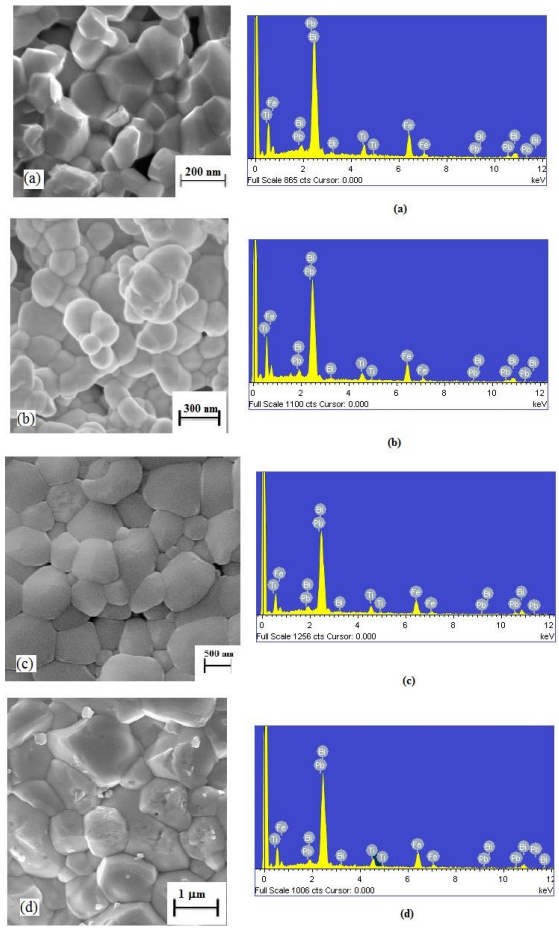

Fig. 2.17 Scanning electron micrographs and EDX spectra of BF -0.25PT powder sintered at (a) 700℃ (b) 800℃ (c) 900℃ (d) 1000℃.

Table 2.5 Results of EDX analysis of BF-0.25PT samples with different sizes.

Element	Estimated sizes BF-0.25PT from SEM			
	Clacined at 700℃	Sintered at 800℃	Sintered at 900℃	Sintered at 1000℃
	150nm	300 nm	500 nm	2μm
	Atomic(%) from EDX			
Bi	42.03	42.15	42.50	42.05
Fe	32.71	33.02	32.61	33.30
Pb	10.04	10.46	10.74	11.37
Ti	15.21	14.37	14.15	13.27
BF:PT	74.74:25.24	75.17:24.83	75.11:24.89	75.35:24.64

2.12.6 Microstructural and compositional studies for BF-0.20PT

The average size and sintering temperatures are given in Table 2.6. The minimum particle size has been found to be ~180 nm for sample sintered at 700℃, whereas the largest size is ~2.1μm corresponding to the sintering temperatures of 1000 ^{0}C. Representative EDX spectrum of each sample is shown on the right side column of SEM image. Its analysis confirmed that the average composition composition of all the sizes within accepted limit.

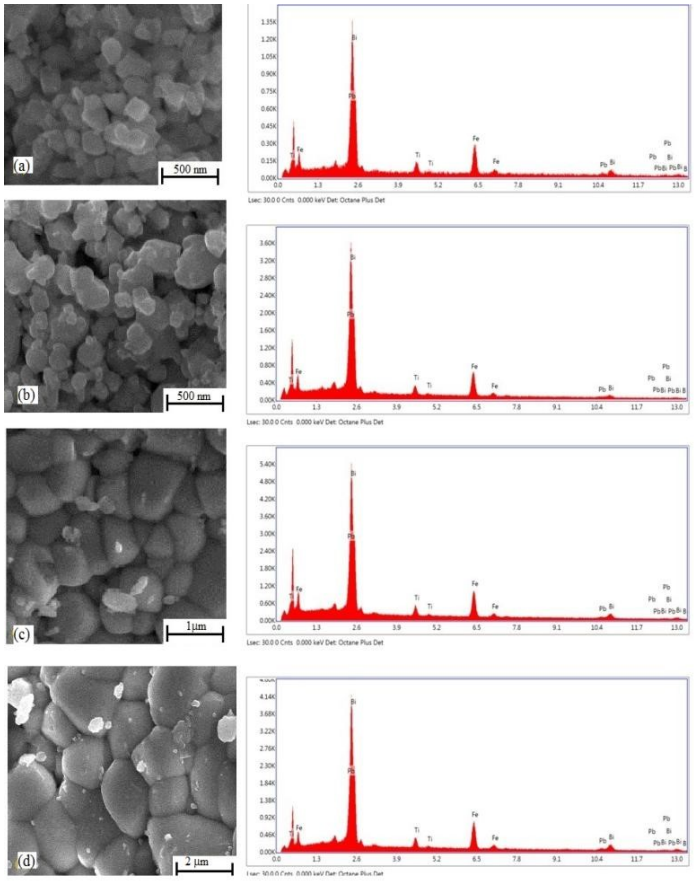

Fig. 2.18 Scanning electron micrographs and EDX spectra of BF -0.20PT powder sintered at (a) 700℃ (b) 800℃ (c) 900℃ (d) 1000℃

Table 2.6 Results of EDX analysis of BF-0.20PT samples with different sizes.

Element	Estimated sizes BF-0.20PT from SEM			
	Clacined at 700℃	Sintered at 800℃	Sintered at 900℃	Sintered at 1000℃
	180nm	350 nm	700 nm	2.1μm
	Atomic(%) from EDX			
Bi	58.79	60.39	58.96	58.82
Fe	21.50	19.96	21.27	21.56
Pb	14.64	15.05	15.06	14.95
Ti	5.07	4.60	4.81	4.67
BF:PT	80.29:19.71	80.35:19.65	80.23:19.77	80.38:19.62

2.12.7 Microstructural and compositional studies for BF-xPT (x=0.2, 0.25 and 0.30) calcined at 550℃

The average particle sizes of calcined samples are given in Table 2.7. As we can see from table that average size increases with decreasing concentration of $PbTiO_3$. Representative EDX spectrum of each sample is shown on the right side column of SEM image. Its analysis confirmed that the average composition of all the sizes within accepted limit.

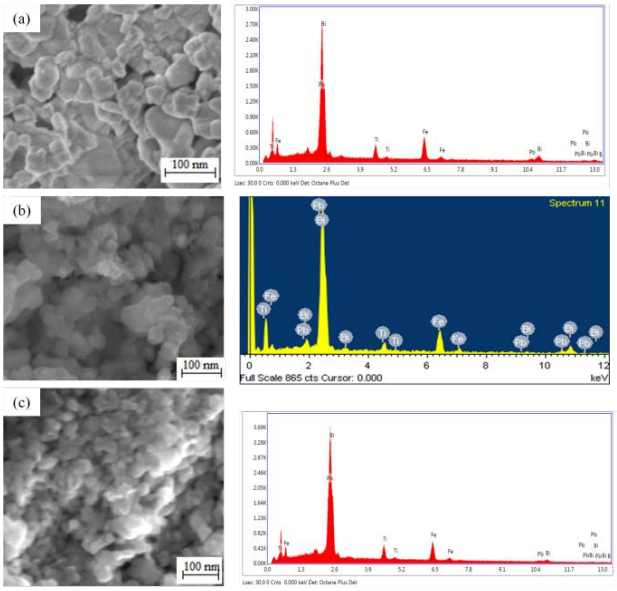

Fig. 2.19 Scanning electron micrographs and EDX spectra of (a)BF-0.20PT, (b) BF-0.25PT and (c) BF-0.30PT powder calcined at 550℃.

Table 2.7 Results of EDX analysis

Element	Estimated sizes of calcined powder from SEM		
	BF-0.20PT	BF-0.25PT	BF-0.30PT
	70nm	50 nm	45 nm
	Atomic(%) from EDX		
Bi	59.79	42.13	50.37
Fe	20.08	32.71	19.42
Pb	15.14	10.14	22.51
Ti	4.27	15.02	7.70
BF:PT	80.59:19.41	74.84:25.16	69.79:30.21

2.8 Conclusion

All the compositions of BF-xPT ($0.20 \leq x \leq 0.50$) solid solution were successfully synthesized by sol-gel method. The synthesized sample were almost free from all impurity phases such as $Bi_2Fe_4O_9$, $Bi_{25}FeO_{39}$ which are commonly formed during the different stages of synthesis. The average grains size of the powders synthesized by this method are in the range 18nm to 2.1μm. EDX analysis confirms that stoichiometric compositions were formed with in the accepted limit of EDX.

The average grain size was found to effectively growing with increasing $BiFeO_3$ content.

Sintering Temp.	x=0.20 (nm)	x=0.25 (nm)	x=0.30 (nm)	x=0.35 (nm)	x=0.40 (nm)	x=0.50 (nm)
1000/1050℃	2100	2000	1000	750	350	120
900/950℃	700	500	380	300	110	45
800/850℃	350	300	220	150	60	31
700/750℃	180	150	100	-	-	21
550℃ (Calcined)	70	50	45	42	40	18

We have taken the crystallographic studies on these samples in the net chapter.